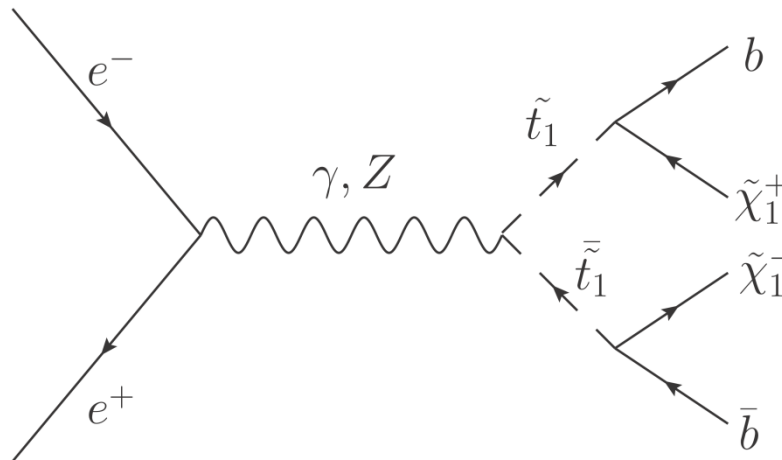


Production of stops in $e^+ e^-$ annihilation close to threshold

Peter Poier

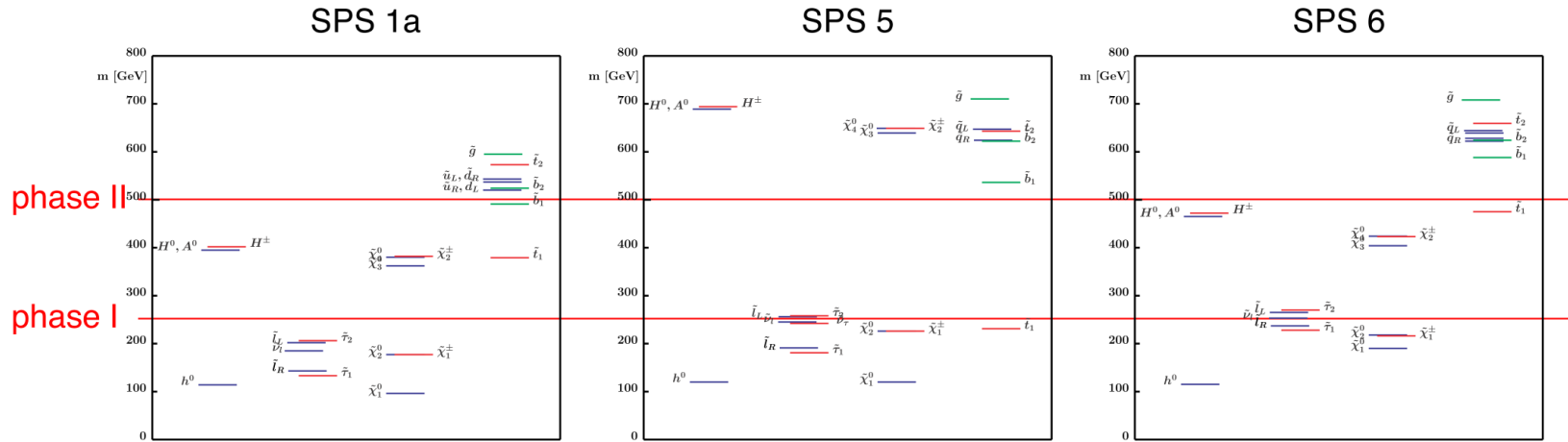
in collaboration with André H. Hoang and Pedro Ruiz-Femenía
University of Vienna

April 19, 2012



Motivation:

In many SUSY models stop pair production is possible at the ILC:



$$m_{\tilde{t}_1} = 396 \text{ GeV}$$

$$\tilde{t}_1 \rightarrow b\chi_1^+, \dots$$

$$\Gamma_{\tilde{t}_1} = 1.92 \text{ GeV}$$

$$m_{\tilde{t}_1} = 240 \text{ GeV}$$

$$\tilde{t}_1 \rightarrow b\chi_1^+, c\chi_1^0$$

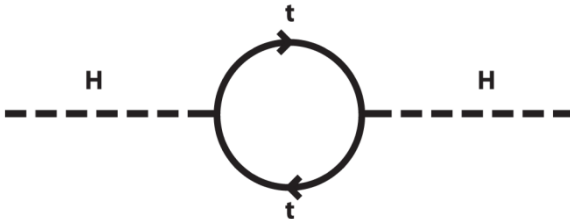
$$\Gamma_{\tilde{t}_1} = 0.04 \text{ GeV}$$

$$m_{\tilde{t}_1} \simeq 490 \text{ GeV}$$

$$\tilde{t}_1 \rightarrow b\chi_1^+, \dots$$

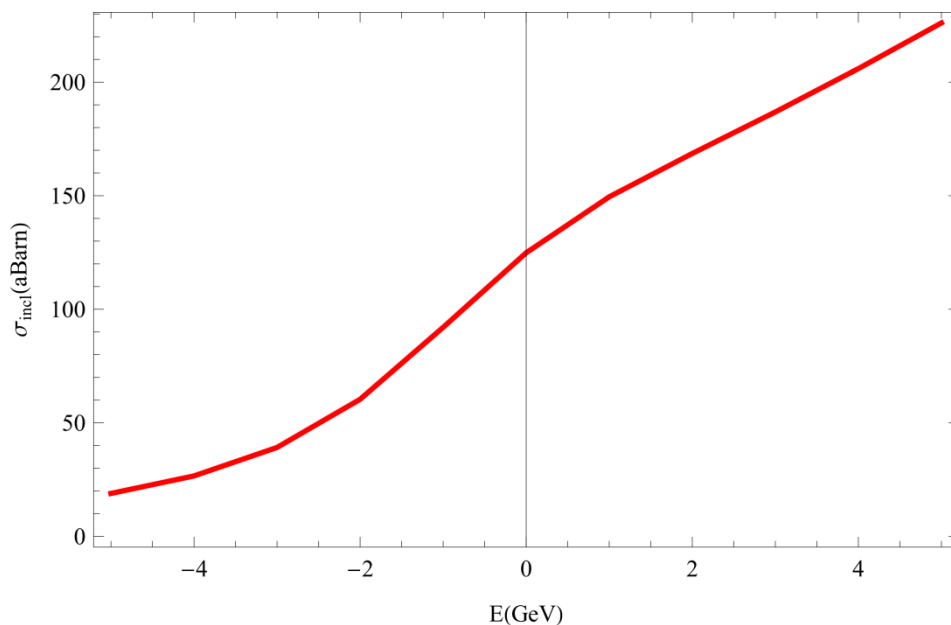
$$\Gamma_{\tilde{t}_1} \simeq 3.2 \text{ GeV}$$

Stop mass is supposed to be small



Motivation:

Threshold scan:



determine:

$$m, y_{\tilde{t}_1}, \Gamma_{\tilde{t}_1}$$

Precision aim:

$$\frac{\sigma(e^+e^- \rightarrow \tilde{t}_1\bar{\tilde{t}}_1)}{\sigma(e^+e^- \rightarrow t\bar{t})} \sim v^2 \sim \frac{1}{100} \Rightarrow \frac{\Delta\sigma(e^+e^- \rightarrow \tilde{t}_1\bar{\tilde{t}}_1)}{\sigma(e^+e^- \rightarrow \tilde{t}_1\bar{\tilde{t}}_1)} \sim 10 \frac{\Delta\sigma(e^+e^- \rightarrow t\bar{t})}{\sigma(e^+e^- \rightarrow t\bar{t})} \sim 10 - 20\%$$

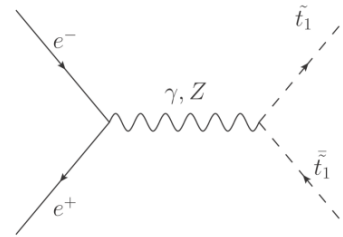
Outline:

- 1-loop calculation
- EFT framework and factorization
- PS matching
- Comparison to Monte Carlo simulation, Results

1-Loop calculation

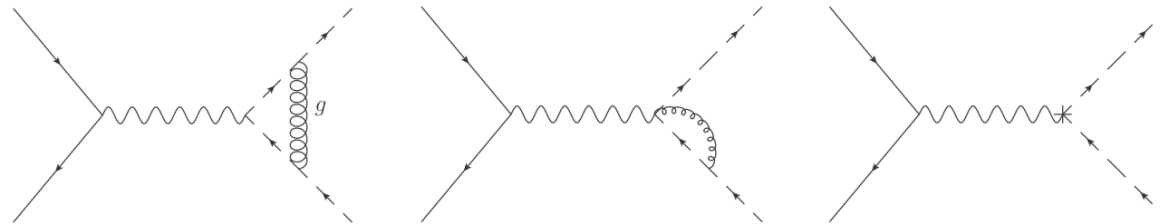
Diagrams contributing to $\sigma(e^+e^- \rightarrow \tilde{t}_1\tilde{t}_1^*)$ at 1-loop order (neglecting electroweak corrections):

Tree level diagram:



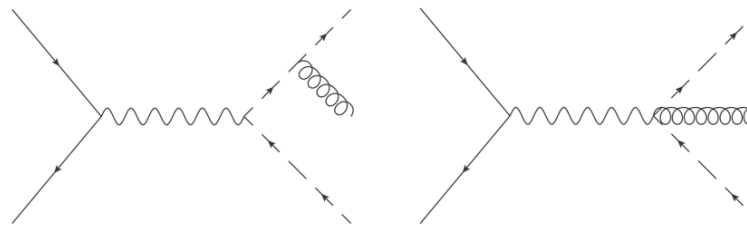
(a)

Virtual corrections:



(b)

Real radiation:



(c)

Effect of the vertex correction

Tree level vertex:

$$\begin{array}{c} \tilde{t}_1 \\ \diagup \\ \mu \text{ --- } \gamma, Z \\ \diagdown \\ \tilde{t}_1 \end{array} = -ie_0 \tilde{Q}_{\gamma/Z} (p_{\tilde{t}_1} - p_{\tilde{t}_1})^\mu$$

1-loop level vertex:

$$\Gamma^\mu \equiv -ie_0 \tilde{Q}_{\gamma/Z} (p_{\tilde{t}_1} - p_{\tilde{t}_1})^\mu F(q^2) = \begin{array}{c} \tilde{t}_1 \\ \diagup \\ \mu \text{ --- } \gamma, Z \\ \diagdown \\ \tilde{t}_1 \end{array} \bullet$$

$$= \begin{array}{c} \tilde{t}_1 \\ \diagup \\ \mu \text{ --- } \gamma, Z \\ \diagdown \\ \tilde{t}_1 \end{array} + \begin{array}{c} \tilde{t}_1 \\ \diagup \\ \text{---} \\ \diagdown \\ \tilde{t}_1 \end{array} + \begin{array}{c} \tilde{t}_1 \\ \diagup \\ \text{---} \\ \diagdown \\ \tilde{t}_1 \end{array} + \begin{array}{c} \tilde{t}_1 \\ \diagup \\ \text{---} \\ \diagdown \\ \tilde{t}_1 \end{array} + \begin{array}{c} \tilde{t}_1 \\ \diagup \\ \text{---} \\ \diagdown \\ \tilde{t}_1 \end{array}$$

Virtual correction to the cross-section:

$$|F|^2 = |1 + \delta F|^2 = 1 + 2\text{Re}(\delta F) + O(\alpha_S^2)$$

$$\sigma(e^+e^- \rightarrow \tilde{t}_1 \tilde{t}_1) = \sigma^{(\text{tree})} + \delta\sigma^{(\text{virtual})} = (1 + 2\text{Re}\delta F)\sigma^{(\text{tree})}$$

↑ includes IR divergences

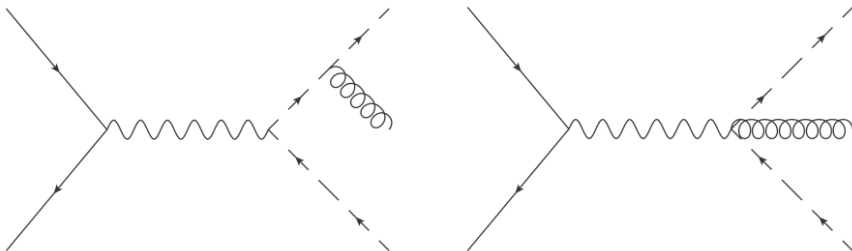
← $O(\epsilon)$ term needed!

I.R. divergences in $\sigma(e^+e^- \rightarrow \tilde{t}_1\tilde{t}_1^*) = (1 + 2Re\delta F)\sigma^{(tree)}$

$$2Re \delta F = C_F \frac{\alpha_S}{\pi} \left[\frac{(1 + \beta^2)}{\beta} \left(\frac{\log(w)}{2\epsilon_{IR}} - \frac{1}{2} \log(w) \log\left(\frac{\mu_{IR}^2}{m^2}\right) + Li_2(w) \right. \right. \\ \left. \left. - \frac{1}{4} \log^2(w) + \log(1-w) \log(w) - \log(w) + \frac{\pi^2}{3} \right) \right. \\ \left. - \frac{1}{\epsilon_{IR}} - \log\left(\frac{\mu_{IR}^2}{m^2}\right) - 2 \right]. \quad \beta = \sqrt{1 - \frac{4m}{q^2}} \text{ and } w = \frac{1-\beta}{1+\beta}$$

$\sigma(e^+e^- \rightarrow \tilde{t}_1\tilde{t}_1^*)$ **virtual** + $\sigma(e^+e^- \rightarrow \tilde{t}_1\tilde{t}_1^* g_{soft})$ **real** is free of I.R. divergences!
(Lee-Nauenberg theorem)

Bremsstrahlung diagrams:



1-Loop calculation result

$$\begin{aligned}\sigma^{(1\text{-loop})} &= \sigma\left(e^+e^- \rightarrow \tilde{t}_1\tilde{t}_1\right) + \sigma\left(e^+e^- \rightarrow \tilde{t}_1\tilde{t}_1g\right) \\ &= \sigma^{(\text{tree})} \left(1 + C_F \frac{\alpha_S}{\pi} f(\beta)\right)\end{aligned}\quad \beta = \sqrt{1 - \frac{4m}{q^2}} \text{ and } w = \frac{1-\beta}{1+\beta}$$

$$\begin{aligned}f(\beta) &= \frac{1 + \beta^2}{\beta} \left[\frac{3}{2\beta} + \log(w) \log(1 + w) + 2 \log(w) \log(1 - w) + 4Li_2(w) + 2Li_2(-w) \right] \\ &\quad - 4 \log(1 - w) - 2 \log(1 + w) + \left[3 + \frac{1}{\beta^3} \left(2 - \frac{5}{4}(1 + \beta^2)^2 \right) \right] \log(w) \\ &= \frac{\pi^2}{2\beta} + O(\beta)\end{aligned}$$

$$\sigma^{(1\text{-loop})} = \sigma^{(\text{tree})} \left(1 + \frac{C_F \pi \alpha_S}{2 \beta} + O(\alpha_S \beta^0) \right)$$

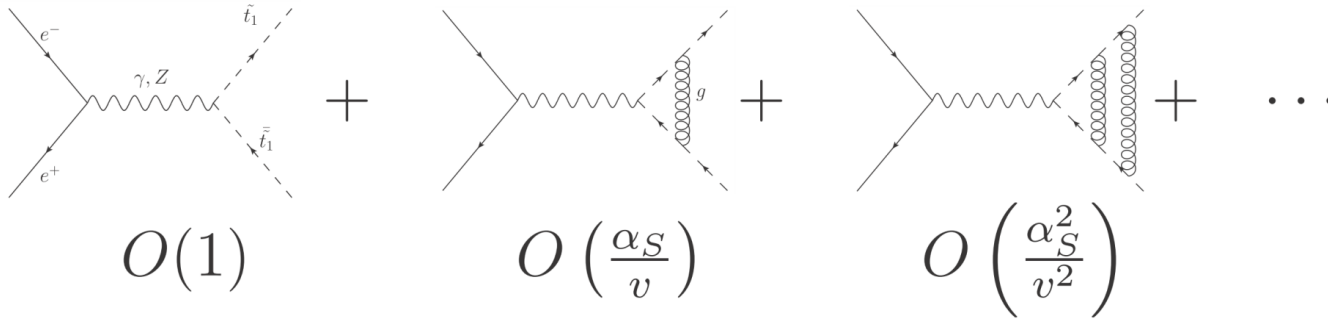
no convergence for $\alpha_S \sim \beta$

Motivation for applying vNRQCD

Problem of Coulomb singularities:

$$\alpha_S \sim v \rightarrow$$

NRQCD



Problem of large logarithms:

3 scales

$$m \text{ (hard)} \gg \vec{p} \sim mv \text{ (soft)} \gg E \sim \Gamma \sim mv^2 \text{ (usoft)} (\gg \Lambda_{\text{QCD}})$$

$$\ln\left(\frac{m^2}{\mathbf{p}^2}\right), \ln\left(\frac{m^2}{E^2}\right), \ln\left(\frac{\mathbf{p}^2}{E^2}\right)$$

→ two correlated renormalization scales:

$$\mu_S = m\nu, \mu_U = m\nu^2, \nu \sim v$$

v'NRQCD

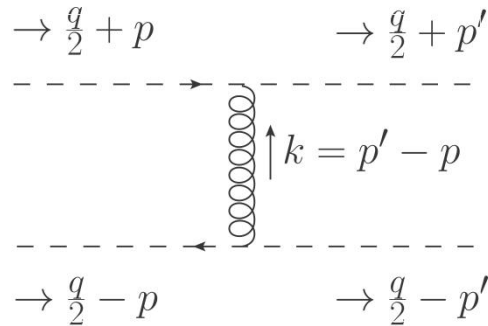
→ RGEs resum $[\alpha_S \ln v]^n$, $\alpha_S [\alpha_S \ln v]^n$, $\alpha_S^2 [\alpha_S \ln v]^n$, ... terms

LL

NLL

NNLL

Expansion of the Gluon propagator in the potential regime:



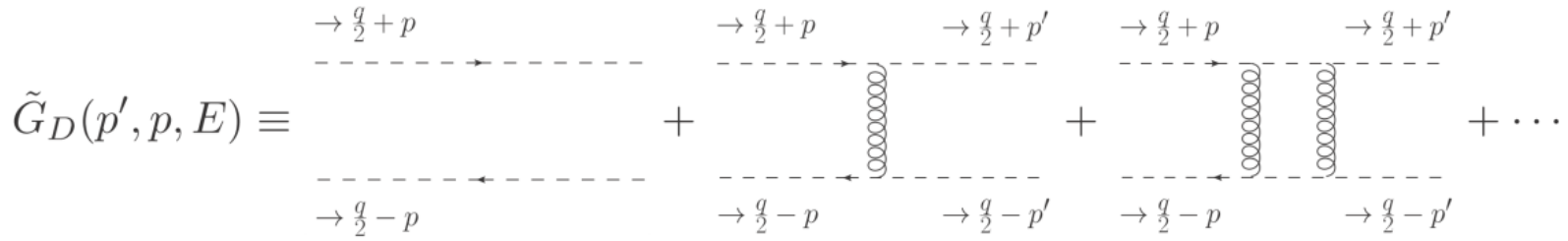
potential: $(k^0, \mathbf{k}) \sim (mv^2, mv)$

$$\frac{-i}{(p - p')^2 + i\epsilon} = \frac{-i}{\underbrace{(p^0 - p'^0)^2}_{\ll (\mathbf{p} - \mathbf{p}')^2} - (\mathbf{p} - \mathbf{p}')^2 + i\epsilon} \approx \frac{i}{(\mathbf{p} - \mathbf{p}')^2 - i\epsilon} \sim \tilde{V}_C(|\mathbf{p} - \mathbf{p}'|)$$

$$V_C(r) \equiv -\frac{a}{r}$$

Expansion for the Gluon propagator in the potential regime gives the Fourier transform of the Coulomb potential

Summing up ladder diagrams:



Green's function of the Schrödinger equation

$$V_C(r) \equiv -\frac{a}{r}$$

$$\left(-\frac{\nabla_{\mathbf{x}'}^2}{m} + V_C(x') - (E + i\Gamma_{\tilde{t}_1}) \right) G_C(\mathbf{x}', \mathbf{x}, E) = \delta^3(\mathbf{x}' - \mathbf{x})$$

$$\tilde{G}_C(\mathbf{p}', \mathbf{p}, E) \equiv \int d^3\mathbf{x}' d^3\mathbf{x} e^{-i\mathbf{p}' \cdot \mathbf{x}'} G_C(\mathbf{x}', \mathbf{x}, E) e^{i\mathbf{p} \cdot \mathbf{x}}$$

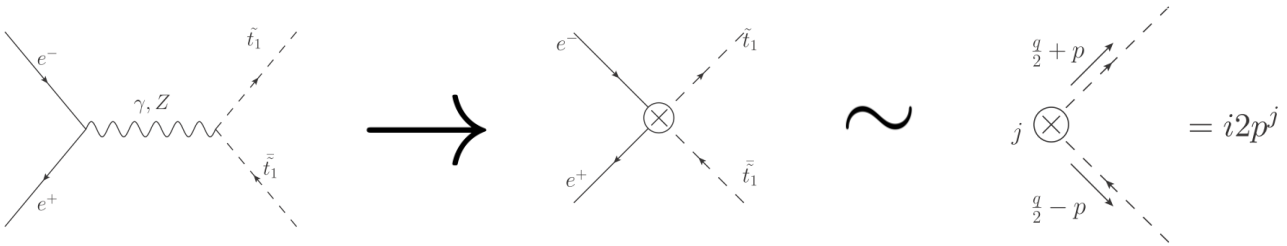
Connection between Green's function and the sum of ladder diagrams

$$\tilde{G}_D(p', p, E) \approx f(p') (-i) \tilde{G}_C(\mathbf{p}', \mathbf{p}, E) f(p)$$

$$f(p) \equiv \frac{i}{\frac{E}{2} + p^0 - \frac{\mathbf{p}^2}{2m} + i\frac{\Gamma_{\tilde{t}_1}}{2}} + \frac{i}{\frac{E}{2} - p^0 - \frac{\mathbf{p}^2}{2m} + i\frac{\Gamma_{\tilde{t}_1}}{2}}$$

Factorization:

$\tilde{t}_1 \tilde{t}_1^*$ production vertex



p-wave Green's function

$$\begin{aligned}
 & \text{Diagram 1} + \text{Diagram 2} + \text{Diagram 3} + \dots \sim \int \frac{d^3 p'}{(2\pi)^3} \frac{d^3 p}{(2\pi)^3} p'^l \tilde{G}_C(\mathbf{p}', \mathbf{p}, E) p^k \equiv \tilde{G}_C^P \frac{\delta^{lk}}{3}
 \end{aligned}$$

Optical theorem

$$\sigma_{\text{tot}}(k_1, k_2 \rightarrow \text{anything}) = \frac{\text{Im}(\mathcal{M}_{\text{fwd. scatter}})}{2E_{\text{cm}} p_{\text{cm}}}$$

→ Factorization formula

$$\sigma_{\text{tot}} \sim \text{Im} \left[\text{Diagram 1} + \text{Diagram 2} + \text{Diagram 3} + \dots \right] \sim \text{Im} \left[(C_V^2 + C_A^2) \tilde{G}_C^P \right]$$

PS divergences in $Im\tilde{G}_C^P(E)$

$$\tilde{G}_C^P(E) = \frac{m^4}{4\pi} \left\{ \boxed{iv^3} - av^2 \left[\ln\left(\frac{-iv}{\nu}\right) - 1 + \ln 2 + \gamma_E + \Psi\left(1 - \frac{ia}{2v}\right) \right] \right. \\ \left. + i\frac{va^2}{4} - \frac{a^3}{4} \left[\ln\left(\frac{-iv}{\nu}\right) - \frac{7}{4} + \ln 2 + \gamma_E + \Psi\left(1 - \frac{ia}{2v}\right) \right] \right\} \\ + \frac{m^4}{16\pi} \left(\frac{1}{\epsilon} + \frac{2}{3} \right) \left(v^2 a + \frac{a^3}{8} \right),$$

$$v^2 = \frac{E + i\Gamma}{2m}, \quad a \sim \alpha_S \sim v$$

We assume a finite width $\Gamma \sim E \sim mv^2$

- $\frac{1}{\epsilon}$ divergence in the imaginary part appears at LO
- Even at LO we need additional matching information to compute σ_{tot}
- Divergence is a PS divergence

Comparison to $e^+e^- \rightarrow t\bar{t}$

$$\tilde{G}_C^S(E) \equiv \int \frac{d^3p'}{(2\pi)^3} \frac{d^3p}{(2\pi)^3} \cancel{(\mathbf{p}'\mathbf{p})} \tilde{G}_C(\mathbf{p}', \mathbf{p}, E) \quad , \quad Im\tilde{G}_C^S(E) \text{ is finite!}$$

Invariant mass cut-off:

Possible stop decays (Electroweak decay):

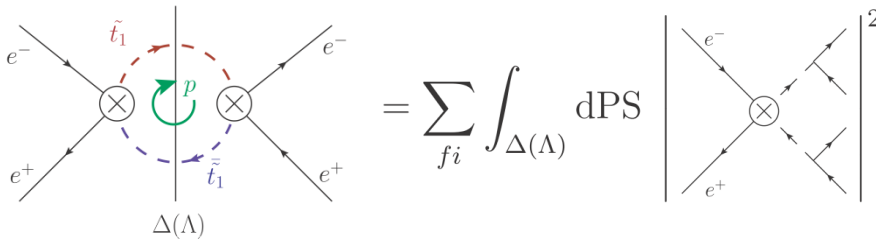
$$\tilde{t}_1 \rightarrow b\tilde{\chi}_j^+, t\tilde{\chi}_j^0$$

Kinematic Cut:

$$M_{\tilde{t}_1}^2 = p_{\tilde{t}_1}^2 = (p_b + p_{\tilde{\chi}_1^+})^2$$

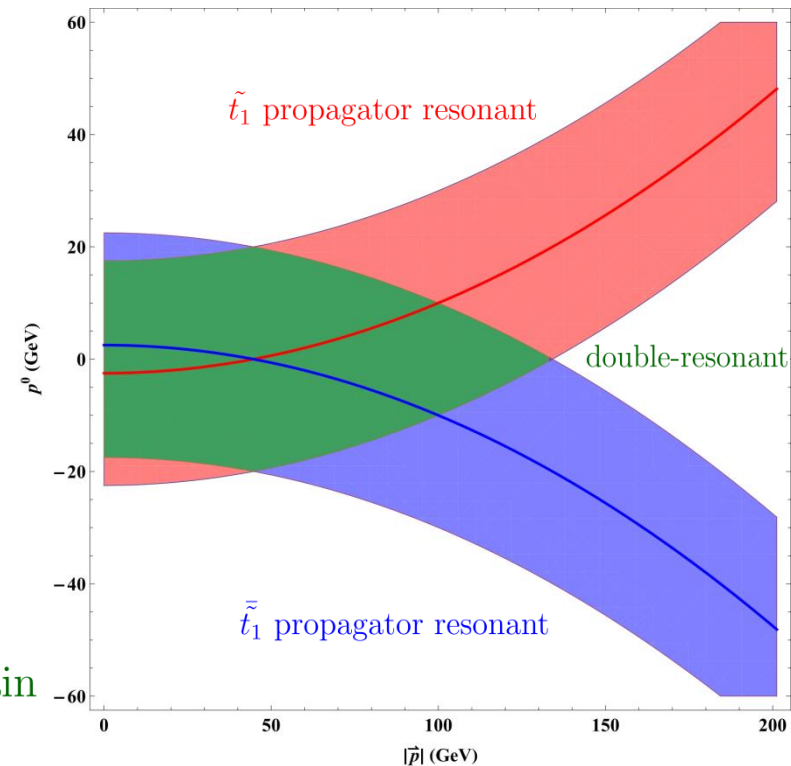
$$|m - M_{\tilde{t}_1}| \leq \Delta M$$

Meaning of Cutkosky cut with invariant mass cutoff:



$$\Lambda = \sqrt{2m\Delta M}$$

p is restricted to the double-resonant integration domain which is adequately described in vNRQCD



Power Counting:

Scale of ΔM and Λ :

$$\Delta M \sim mv$$

$$\Lambda = \sqrt{2m\Delta M} \sim mv^{1/2}$$

- Λ in between **hard** (m) and **soft** (mv) scale
- Physics at $\mathbf{p} \sim \Lambda$ is hard compared to the Physics at the **soft** (mv) scale
→ **PS Matching** → sum up $\ln\left(\frac{\Lambda^2}{\bar{p}^2}\right)$

Definition of LL and NLL:

$$\text{LL} = \left\{ \underbrace{\frac{\Gamma_{\tilde{t}}\Lambda}{m^2}}_{O(v^{5/2})}, \underbrace{v^3 \left(\frac{\alpha_S}{v}\right)^n, \frac{\alpha_S \Gamma_{\tilde{t}_1}}{m} (\alpha_S \ln v)^n \dots}_{O(v^3)} \right\}$$

$$\text{NLL} = \left\{ \underbrace{\frac{\Gamma^2}{m\Lambda}, \frac{v^2\Gamma}{m\Lambda}}_{O(v^{7/2})}, \underbrace{\frac{\alpha_S \Gamma_{\tilde{t}_1}^2}{\Lambda^2}, \frac{\alpha_S \Gamma_{\tilde{t}_1}^2}{\Lambda^2} \left(\frac{\alpha_S}{v}\right)^n \dots}_{O(v^4)} \right\}$$

PS matching:

Result for PS Integral with kinematic cut at $O(\alpha_S^0)$:

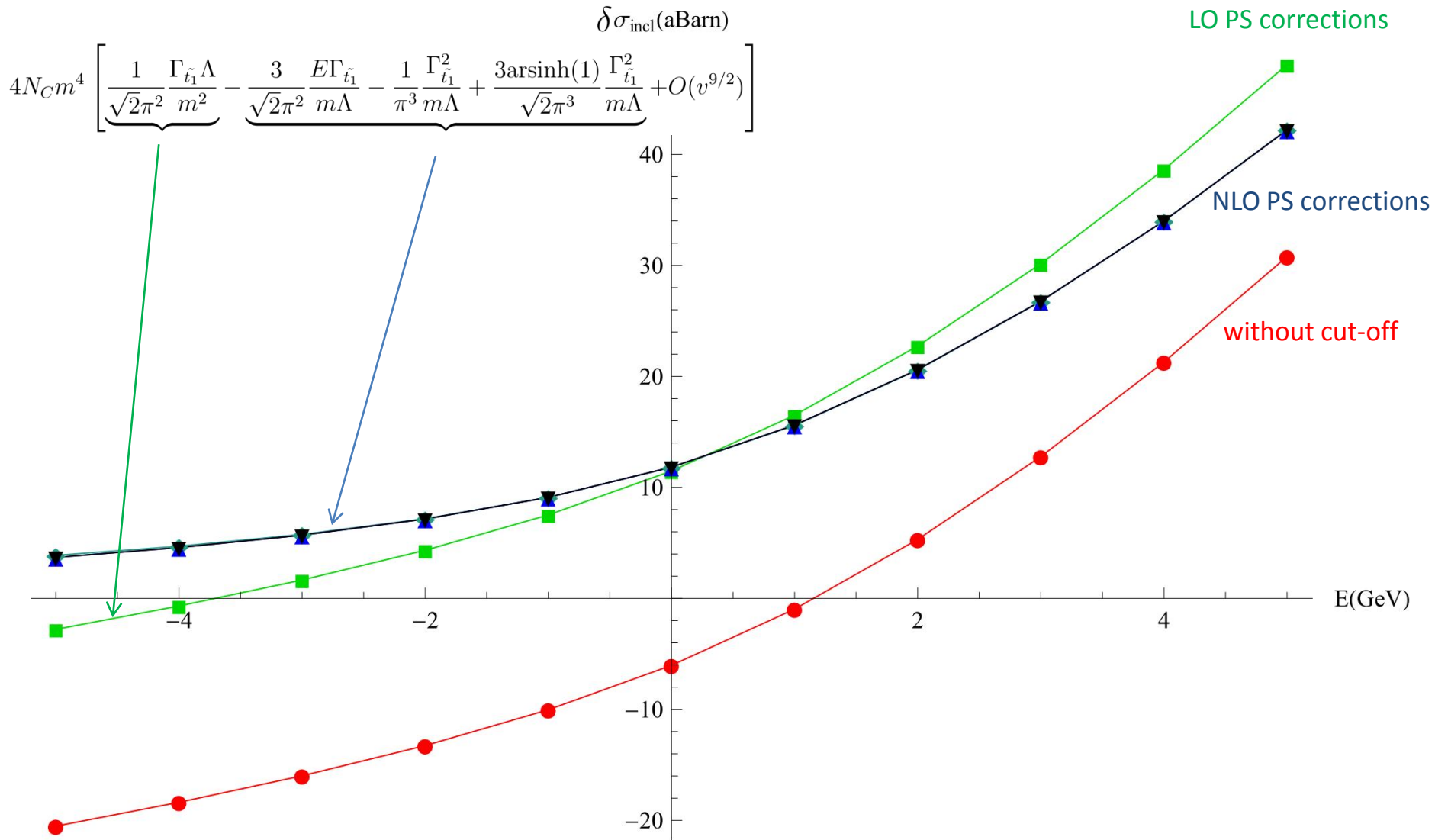
$$\begin{aligned}
 & \text{Diagram with cut} = 2\text{Im} \left[-i \left(\text{Loop Diagram} \right) + 4N_C m^4 \left[\frac{1}{\sqrt{2}\pi^2} \frac{\Gamma_{\tilde{t}_1} \Lambda}{m^2} - \frac{3}{\sqrt{2}\pi^2} \frac{E\Gamma_{\tilde{t}_1}}{m\Lambda} - \frac{1}{\pi^3} \frac{\Gamma_{\tilde{t}_1}^2}{m\Lambda} + \frac{3\text{arsinh}(1)}{\sqrt{2}\pi^3} \frac{\Gamma_{\tilde{t}_1}^2}{m\Lambda} + O(v^{9/2}) \right] \right]
 \end{aligned}$$

We match the effect of the kinematic cut into local operators \rightarrow sum up $\ln\left(\frac{\Lambda^2}{p^2}\right)$

Corresponding expression in EFT with PS matching:

$$2\text{Im} \left[-i \left(\text{Loop Diagram} + \sum_{n=0}^1 \tilde{C}_{V/A,\text{bare}}^{(0,n)}(\Lambda) \left(\text{Tree Diagram} \right) \right) \right]$$

$O(\alpha_S^0)$, $\Delta M = 21\text{GeV}$, $m = 400\text{GeV}$, $\Gamma_{\tilde{t}_1} = 1.2\text{GeV}$



PS matching:

Result for PS Integral with kinematic cut at $O(\alpha_S)$:

$$\Delta(\Lambda) + \Delta(\Lambda) = 2\text{Im} \left[-i \left(\text{diagram with gluon loop on left} \right) \right]$$

$$\frac{4N_C a m^3 \Gamma_{\tilde{t}_1}}{\pi} \left[\frac{1}{3} + \frac{\ln(2)}{4} + \frac{1}{8\epsilon} - \frac{1}{2} \ln \left(\frac{\Lambda}{m\nu} \right) + \frac{Em}{\Lambda^2} - \frac{\Gamma_{\tilde{t}_1} m}{2\pi \Lambda^2} + O(v^2) \right]$$

We match the effect of the kinematic cut into local operators \rightarrow sum up $\ln \left(\frac{\Lambda^2}{p^2} \right)$

Corresponding expression in EFT with PS matching:

$$2\text{Im} \left[-i \left(\text{diagram with gluon loop on left} \right) + \sum_{n=0}^1 \tilde{C}_{V/A,\text{bare}}^{(1,n)}(\Lambda) \left(\text{diagram with single vertex} \right) \right]$$

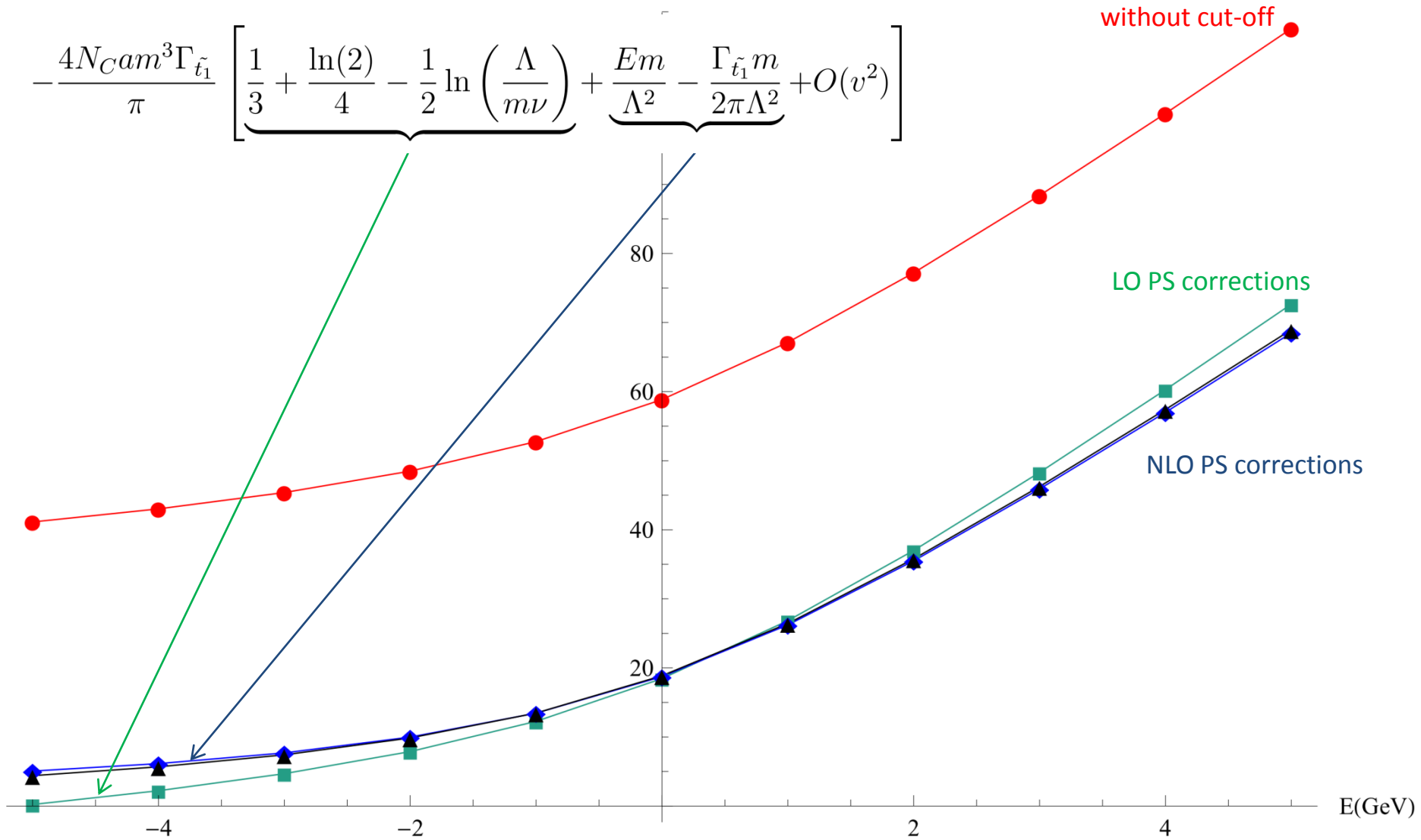
RGE running due to the PS divergence:

$$\frac{d\tilde{C}_{V/A}(\nu)}{d\ln(\nu)} = -i \frac{C_{V/A}(\nu)^2 N_C a(\nu) m^3 \Gamma_{\tilde{t}_1}}{3\pi}$$

$O(\alpha_S)$, $\Delta M = 21\text{GeV}$, $m = 400\text{GeV}$, $\Gamma_{\tilde{t}_1} = 1.2\text{GeV}$

$\delta\sigma_{\text{incl}}(\text{aBarn})$

$$-\frac{4N_C am^3 \Gamma_{\tilde{t}_1}}{\pi} \left[\underbrace{\frac{1}{3} + \frac{\ln(2)}{4} - \frac{1}{2} \ln\left(\frac{\Lambda}{m\nu}\right)}_{\text{LO PS corrections}} + \underbrace{\frac{Em}{\Lambda^2} - \frac{\Gamma_{\tilde{t}_1} m}{2\pi\Lambda^2}}_{\text{NLO PS corrections}} + O(v^2) \right]$$



Full theory expression for a cut propagator:

$$\frac{2mi}{\left(\frac{q}{2} \pm p\right)^2 - m^2 + \Pi} \rightarrow -2\text{Im} \left(\frac{2m}{\left(\frac{q}{2} \pm p\right)^2 - m^2 + \Pi} \right) =$$

$$\frac{2mi}{\left(\frac{q}{2} \pm p\right)^2 - m^2 + \Pi} \left(\frac{2\text{Im}\Pi}{2m} \right) \left(\frac{2mi}{\left(\frac{q}{2} \pm p\right)^2 - m^2 + \Pi} \right)^*$$

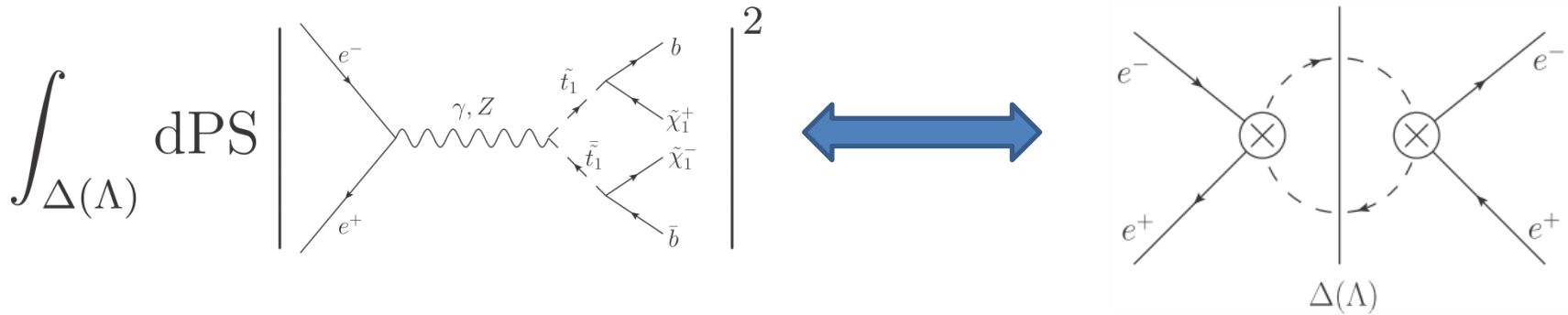
2ImΠ corresponds to a sum of PS integrals:

$$2\text{Im}\Pi(k^2) = \sum_{i=fi} 2\text{Im} \left[-i \begin{array}{c} k \rightarrow \\ \bar{t}_1 \rightarrow \end{array} \begin{array}{c} \text{---} \text{---} \\ \text{---} \text{---} \\ \text{---} \text{---} \end{array} \begin{array}{c} \psi_i \\ \phi_i \end{array} \right]$$

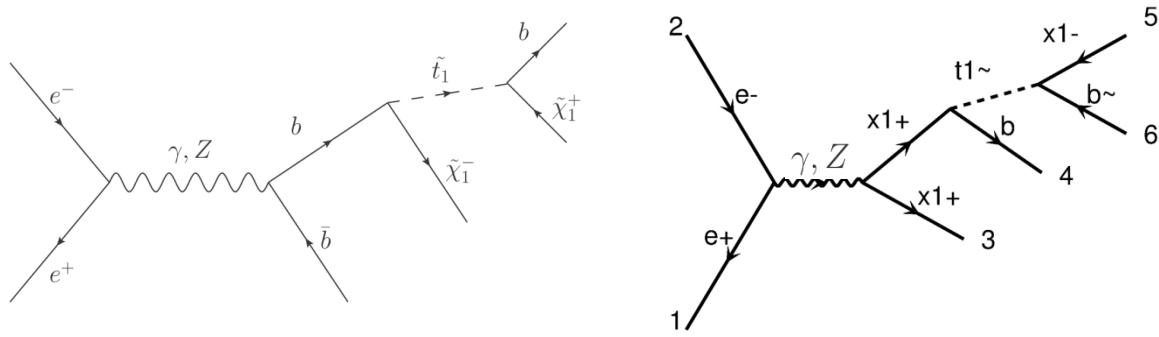
We can restrict us to a specific final state:

$$2\text{Im}\Pi(k^2) \rightarrow 2\text{Im}\tilde{\Pi}(k^2) \equiv 2\text{Im} \left[(-i) \begin{array}{c} k \rightarrow \\ \bar{t}_1 \rightarrow \end{array} \begin{array}{c} \text{---} \text{---} \\ \text{---} \text{---} \\ \text{---} \text{---} \end{array} \begin{array}{c} \tilde{\chi}_i^+ \\ b \end{array} \right] = \text{---} \begin{array}{c} \text{---} \text{---} \\ \text{---} \text{---} \\ \text{---} \text{---} \end{array} \text{---}$$

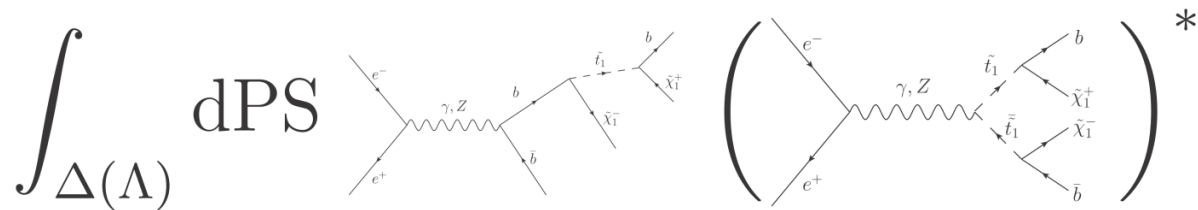
Double-resonant diagrams:



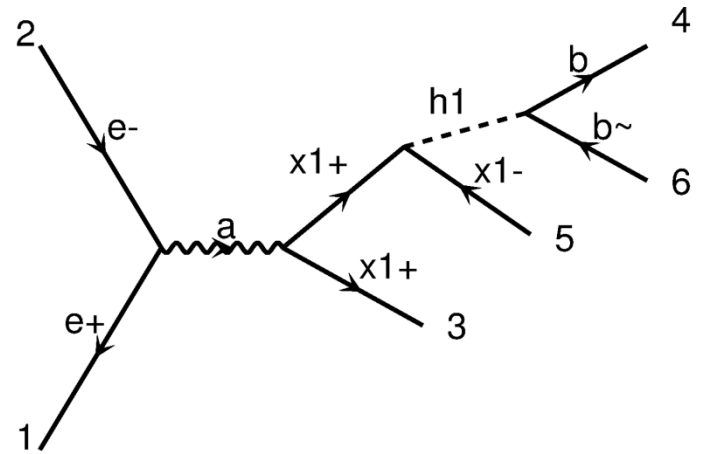
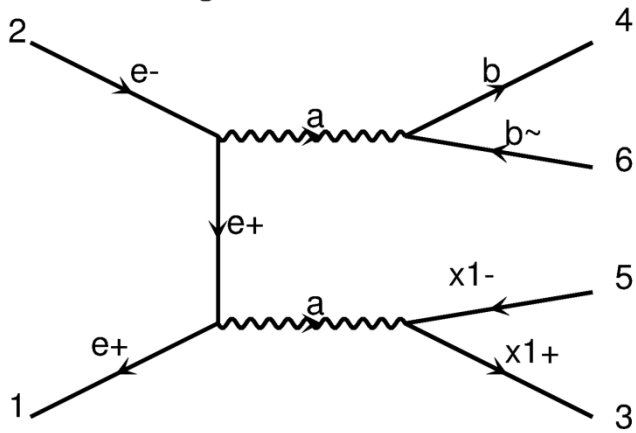
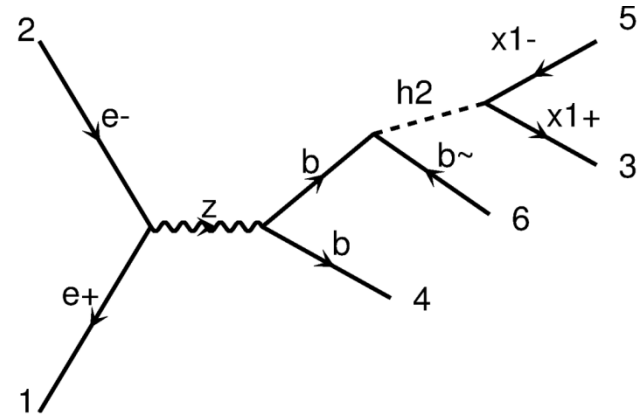
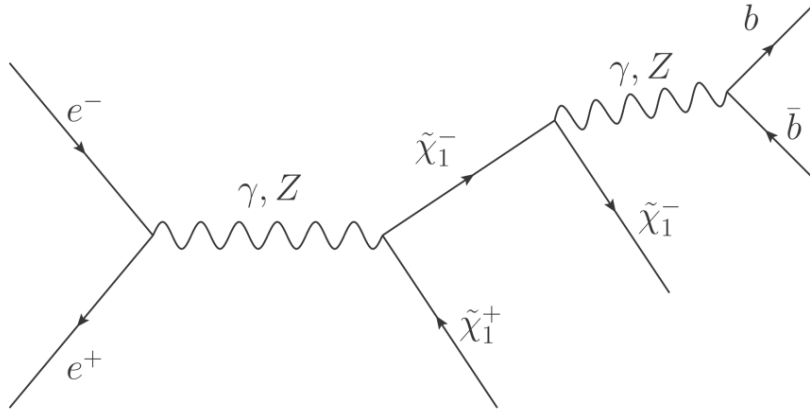
Single-resonant background diagrams:



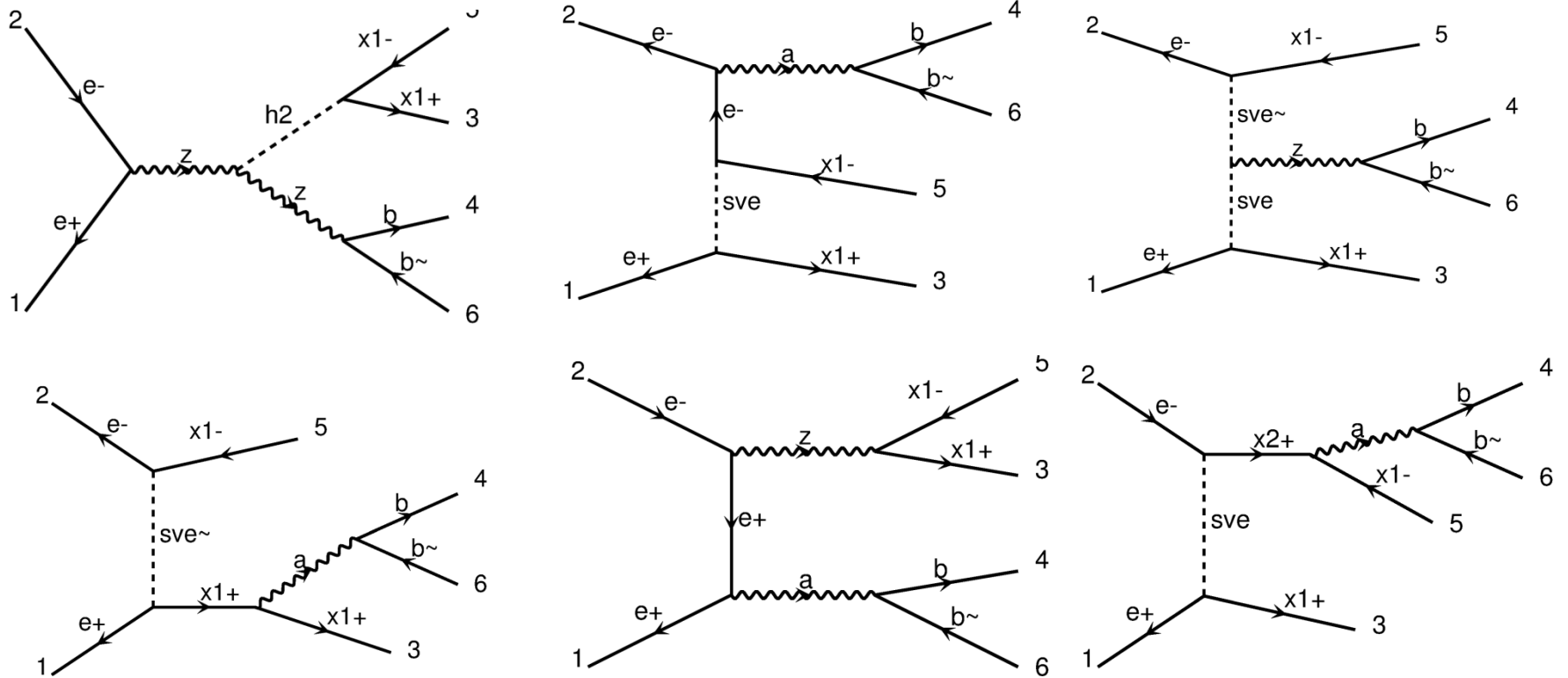
Interference between single and double resonant diagrams:



Non-resonant background diagrams:



Non-resonant background diagrams:



~ 100 non-resonant background diagrams

Contributions to $\sigma_{\text{incl}}(\Lambda)$

$$\sigma_{\text{incl}}(\Lambda) = \sigma_{\text{NRQCD}}(\Lambda) + \sigma_{\text{rem}}(\Lambda)$$

Validation of our method

We approximate σ_{incl} with σ_{NRQCD}

→ it has to be checked that we can find a value for ΔM such that

- Double-resonant contributions are described well in vNRQCD
- Expansion of the effect of the kinematic cut in $\frac{Em}{\Lambda}$, $\frac{\Gamma_{\tilde{t}_1} m}{\Lambda}$ converges
- The contribution of the background (σ_{rem}) is small

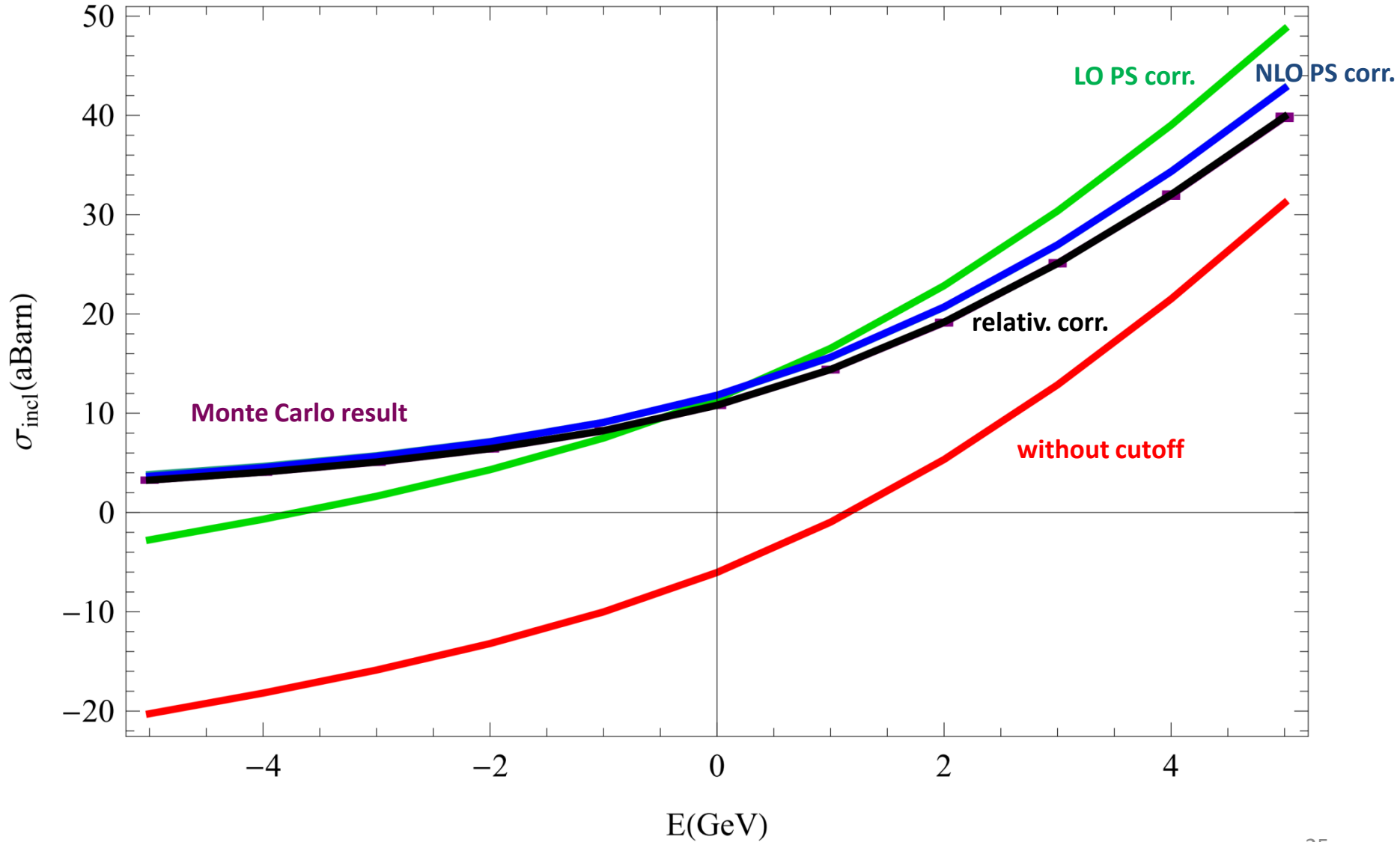
→ we check this with Monte Carlo simulations in Madgraph for

- $e^+e^- \rightarrow \tilde{t}_1 \tilde{t}_1^* \rightarrow b \chi_1^+ \bar{b} \chi_1^-$ (only double-resonant diagrams)
- $e^+e^- \rightarrow b \chi_1^+ \bar{b} \chi_1^-$ (includes background)

Our Monte Carlo simulation is a tree level computation

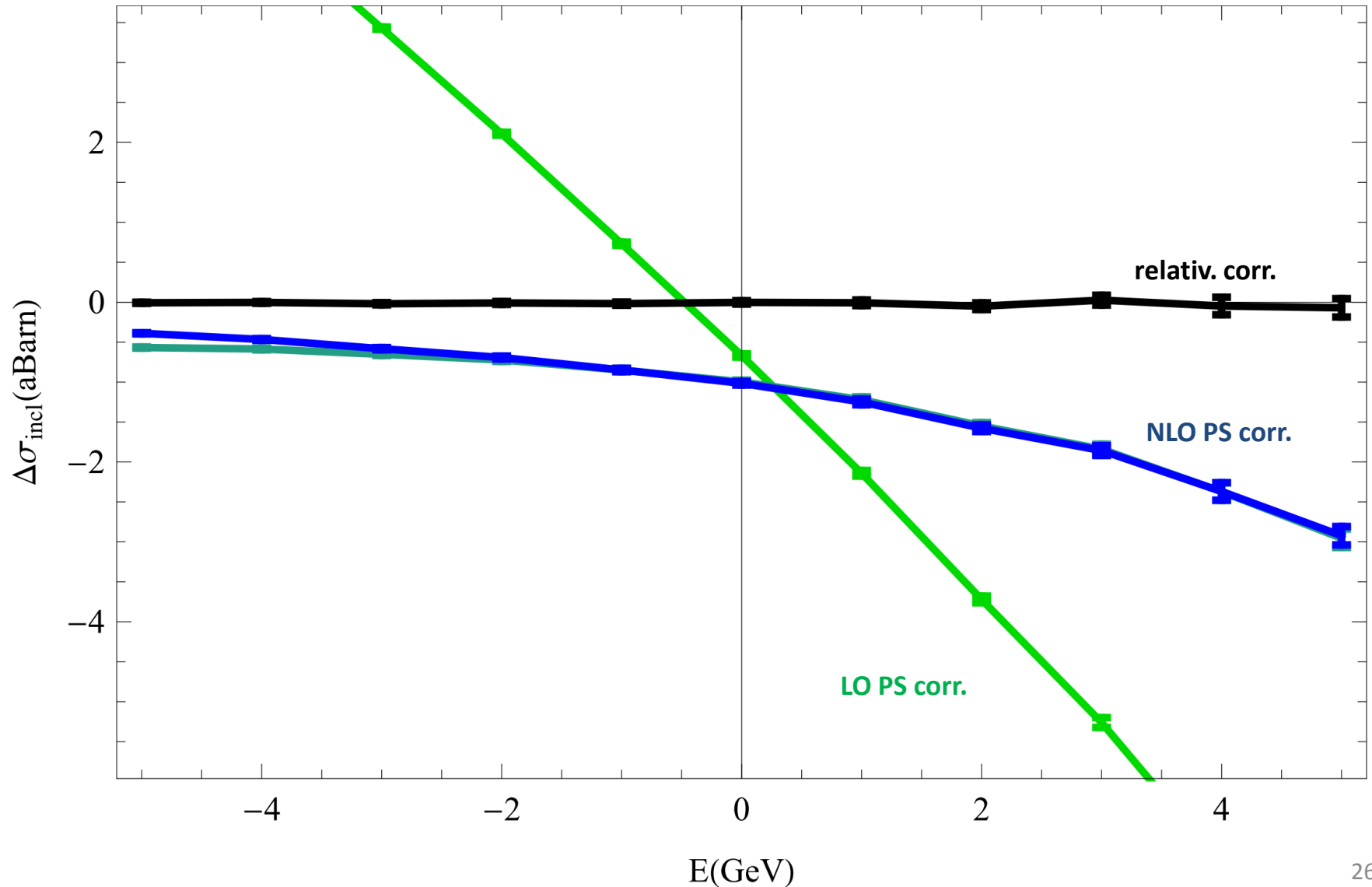
Comparison of our results with a Monte Carlo simulation for $e^+e^- \rightarrow \tilde{t}_1\tilde{t}_1 \rightarrow b\chi_1^+\bar{b}, \chi_1^-$

$O(\alpha_S^0)$, $\Delta M = 21\text{GeV}$, $m = 400\text{GeV}$, $\Gamma(\tilde{t}_1 \rightarrow b\tilde{\chi}_1^+) = 1.2\text{GeV}$



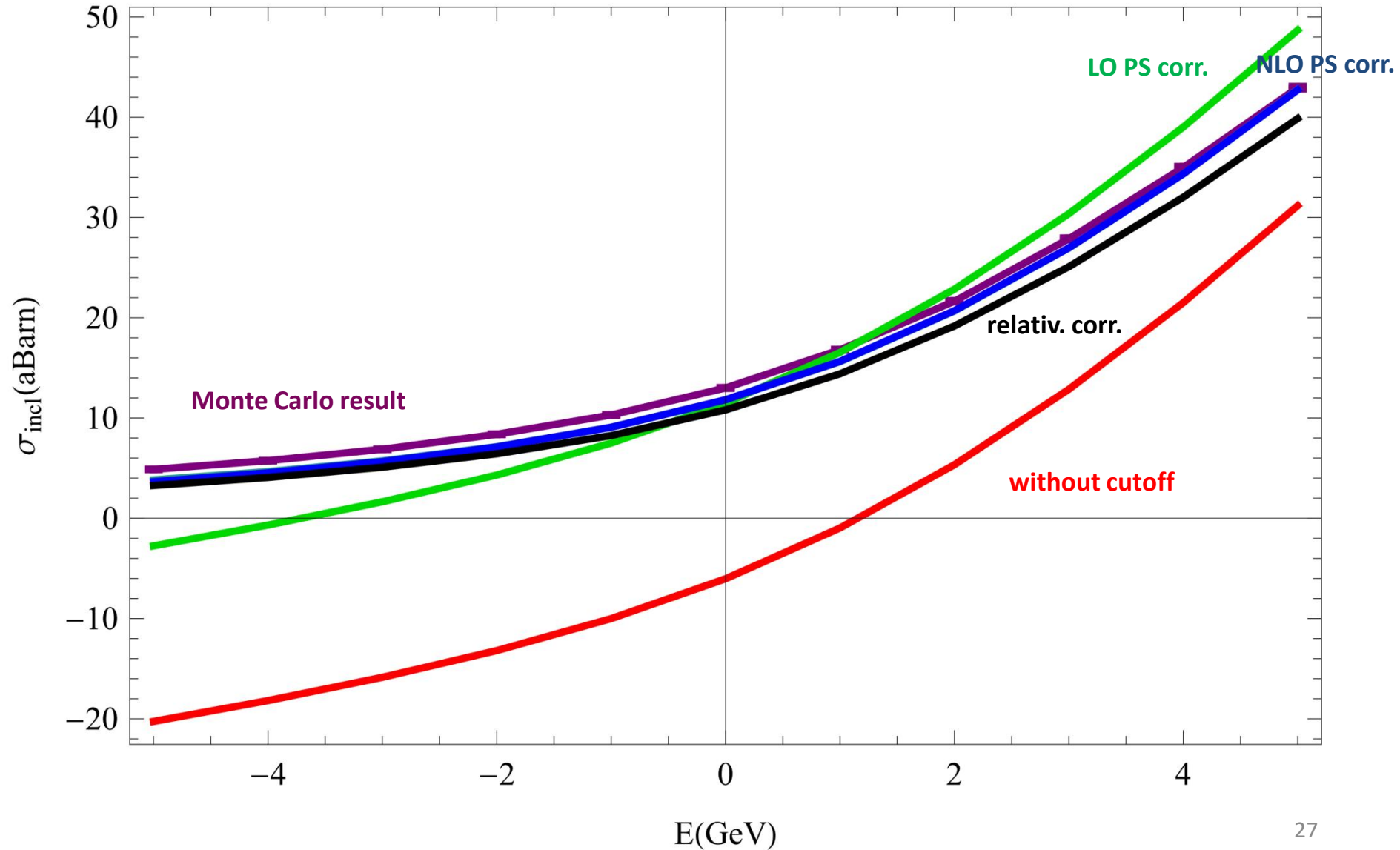
Comparison of our results with a Monte Carlo simulation for $e^+e^- \rightarrow \tilde{t}_1\tilde{t}_1 \rightarrow b\chi_1^+\bar{b}, \chi_1^-$

$O(\alpha_S^0)$, $\Delta M = 21\text{GeV}$, $m = 400\text{GeV}$, $\Gamma(\tilde{t}_1 \rightarrow b\tilde{\chi}_1^+) = 1.2\text{GeV}$



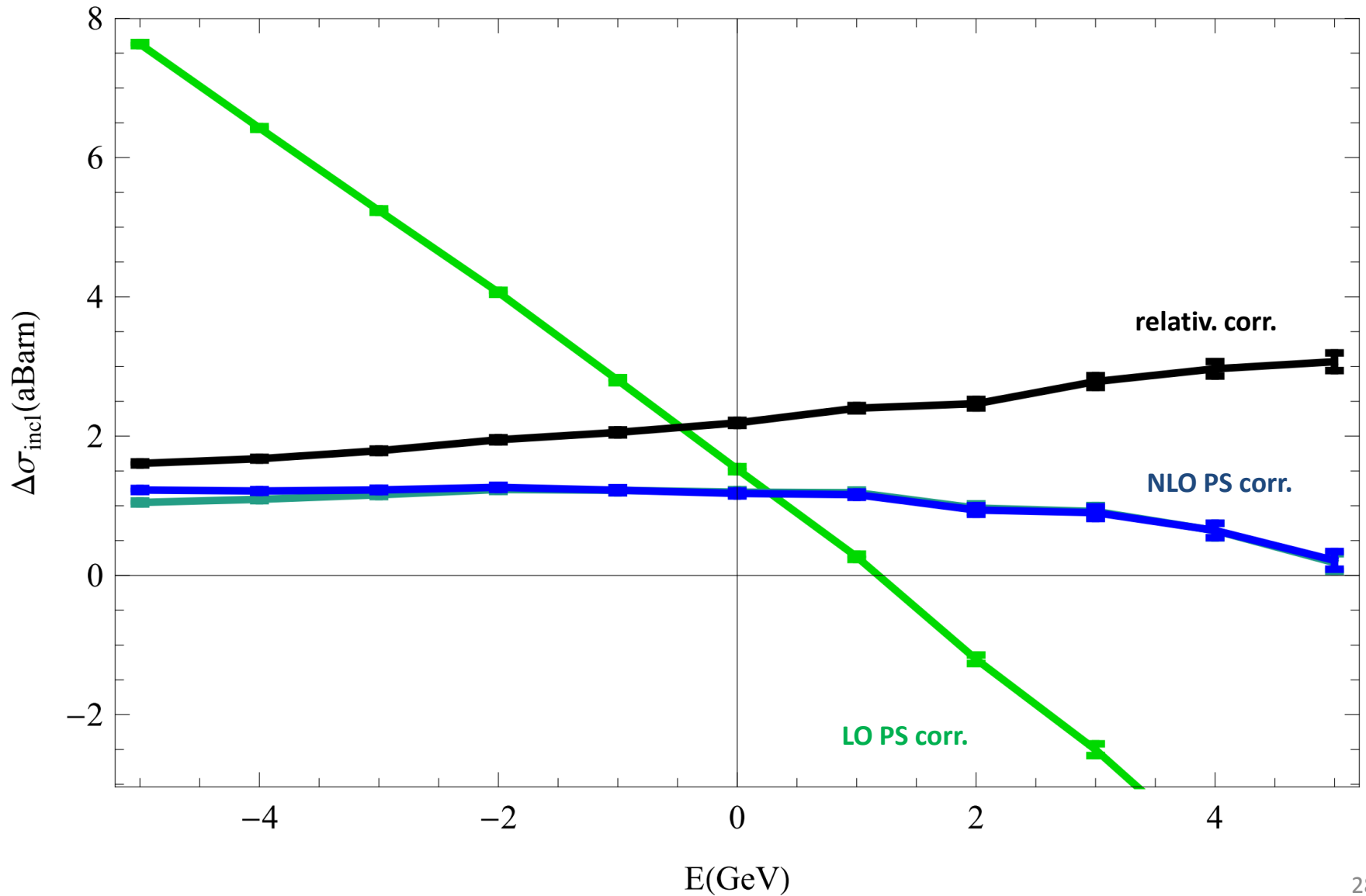
Comparison of our results with a Monte Carlo simulation for $e^+e^- \rightarrow b\chi_1^+\bar{b}, \chi_1^-$

$O(\alpha_S^0)$, $\Delta M = 21\text{GeV}$, $m = 400\text{GeV}$, $\Gamma(\tilde{t}_1 \rightarrow b\tilde{\chi}_1^+) = 1.2\text{GeV}$



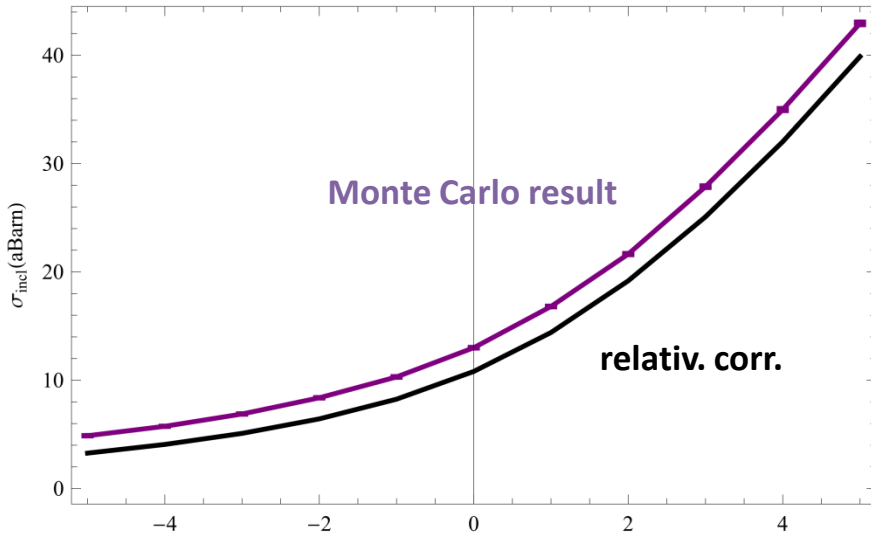
Comparison of our results with a Monte Carlo simulation for $e^+e^- \rightarrow b\chi_1^+\bar{b}, \chi_1^-$

$O(\alpha_S^0)$, $\Delta M = 21\text{GeV}$, $m = 400\text{GeV}$, $\Gamma(\tilde{t}_1 \rightarrow b\tilde{\chi}_1^+) = 1.2\text{GeV}$

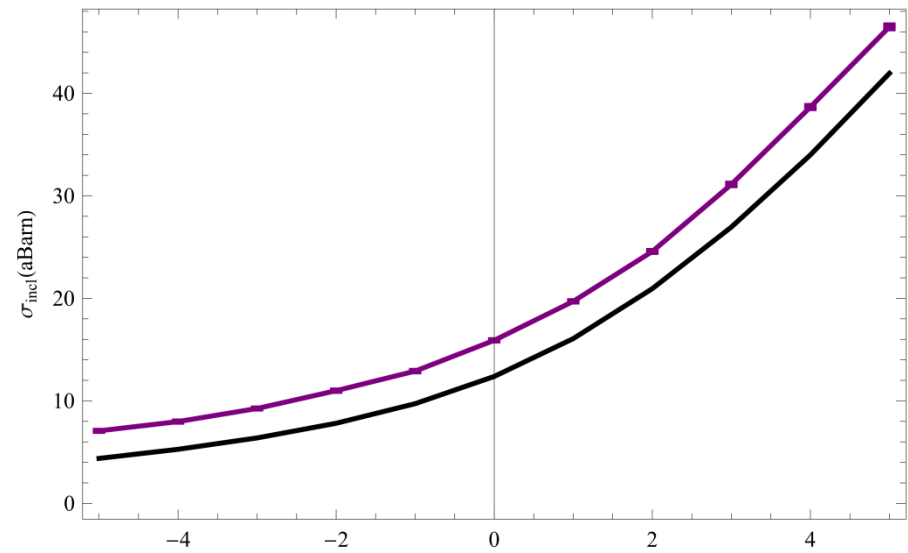


Comparison of our results with a Monte Carlo simulation for $e^+e^- \rightarrow b \chi_1^+ \bar{b}, \chi_1^-$

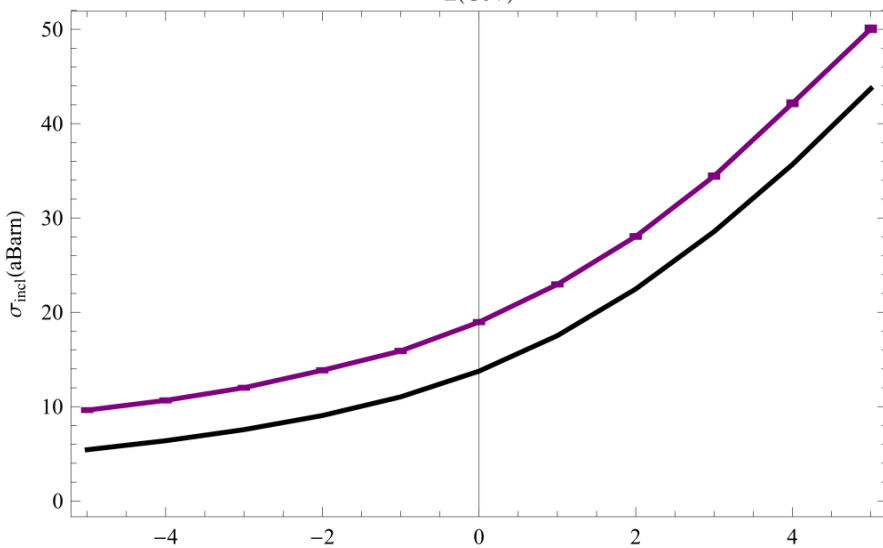
$\Delta M = 21\text{GeV}$



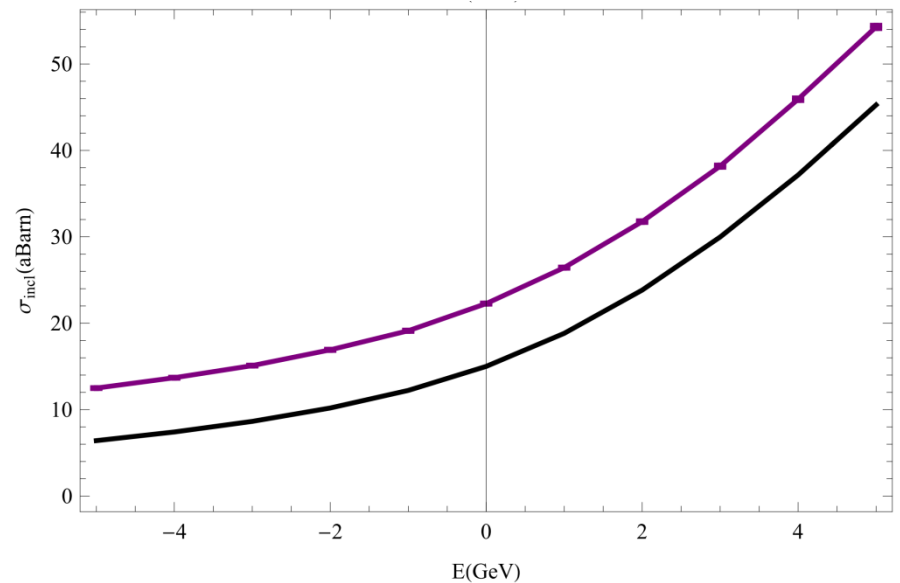
$\Delta M = 26\text{GeV}$



$\Delta M = 31\text{GeV}$



$\Delta M = 36\text{GeV}$

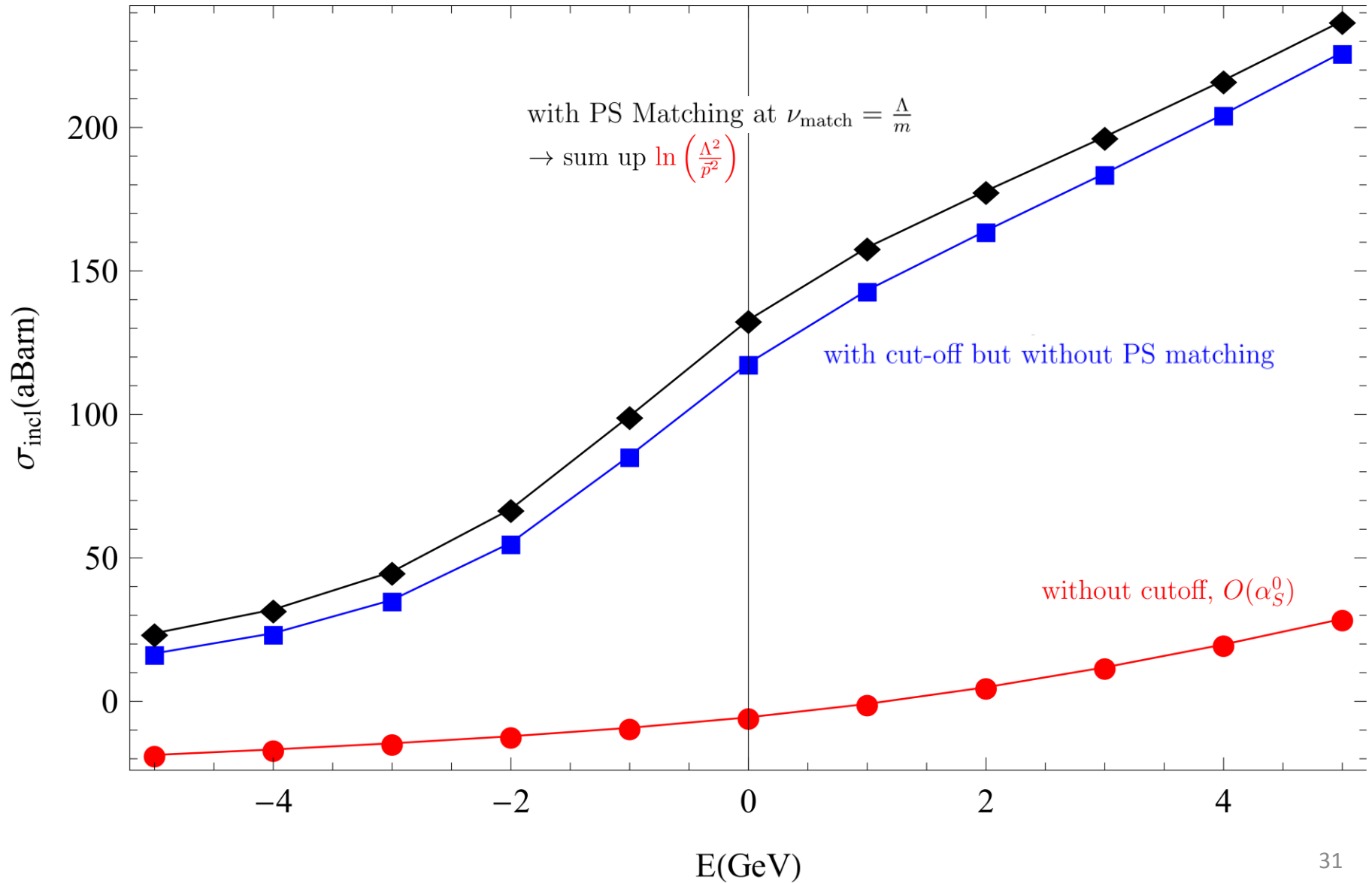


LL result for $e^+e^- \rightarrow b \chi_1^+ \bar{b}, \chi_1^-$

- Match to vNRQCD at $\nu = 1 \rightarrow$ sum up $\ln\left(\frac{m^2}{\mathbf{p}^2}\right)$, $\ln\left(\frac{m^2}{E^2}\right)$, $\ln\left(\frac{\mathbf{p}^2}{E^2}\right)$
- PS Matching at $\nu = \frac{\Lambda}{m} \rightarrow$ sum up $\ln\left(\frac{\Lambda^2}{\bar{p}^2}\right)$
- Apply EFT for $\nu = v$

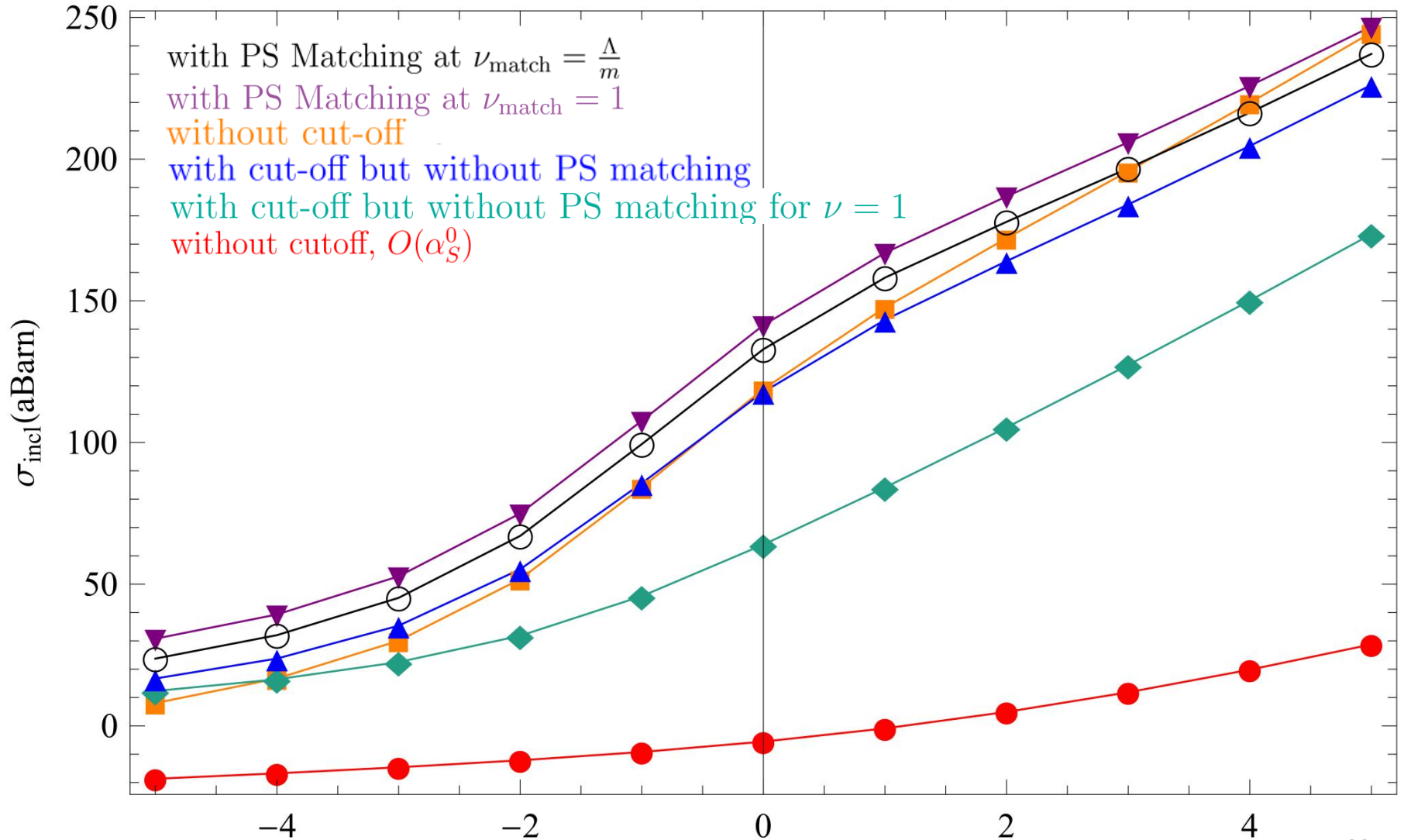
LL result for $e^+e^- \rightarrow b \chi_1^+ \bar{b}, \chi_1^-$

$$\Delta M = 21\text{GeV}, m = 400\text{GeV}, \Gamma(\tilde{t}_1 \rightarrow b\tilde{\chi}_1^+) = 1.2\text{GeV}$$



LL result for $e^+e^- \rightarrow b \chi_1^+ \bar{b}, \chi_1^-$

$\Delta M = 21\text{GeV}, m = 400\text{GeV}, \Gamma(\tilde{t}_1 \rightarrow b\tilde{\chi}_1^+) = 1.2\text{GeV}$



Summary/Outlook:

- Calculation of $\sigma(e^+e^- \rightarrow \tilde{t}_1\tilde{t}_1^*)$ close to threshold
- For $v \sim \alpha_S$ no convergence in expansion in orders of α_S
- PS divergences appear already at LO
- We avoid PS divergences by introducing a kinematic cut on the final states
- We apply PS-matching to sum up logs of the form $\ln\left(\frac{\Lambda^2}{p^2}\right)$
- Compare to $O(\alpha_S^0)$ Monte Carlo simulation for: $e^+e^- \rightarrow b\chi_1^+\bar{b}\chi_1^-$
- Corrections to the Coulomb potential as well as effects of single resonant-diagrams are needed for a full NLL result